# Raman spectroscopy and X-ray diffraction studies on PbO and $(PbO)_{1-x}(TiO_2)_x$



1995 J. Phys.: Condens. Matter 7 8547

(http://iopscience.iop.org/0953-8984/7/45/010)

J. Phys.: Condens. Matter 7 (1995) 8547–8556. Printed in the UK

# Raman spectroscopy and x-ray diffraction studies on PbO and $(PbO)_{1-x}(TiO_2)_x$

A Hedoux†, D Le Bellac‡§, Y Guinet†, J M Kiat‡§, I Noiret† and P Garnier‡‖

† Laboratoire de Dynamique et Structure des Matériaux Moléculaires, URA 801, UFR de Physique, Bâtiment P5, Université de Lille 1, 59655 Villeneuve d'Ascq Cédex, France

‡ Laboratoire de Chimie Physique du Solide, URA 453, Ecole Centrale de Paris, 92295 Chatenay-Malabry Cédex, France

§ Laboratoire Léon Brillouin, CEA Saclay, France

‖ Université d'Evry, Boulevard des Coquibus, 91025 Evry Cédex, France

Received 26 June 1995

**Abstract.** X-ray diffraction and Raman spectroscopy studies of $\alpha$-PBO and $(PbO)_{1-x}(TiO_2)_x$ were performed over a wide temperature range. Investigations on both samples allow us to point out useful information concerning lone-pair interactions from both structural and dynamical points of view. The complementarity of the experimental data gives a better understanding of the phase transition process in PbO, and also of the stability of the tetragonal structure in the solid solution $(PbO)_{1-x}(TiO_2)_x$.

## 1. Introduction

In a previous paper [1], it was shown that the second-order ferroelastic transition at $T_I = 208$ K in $\alpha$-PbO corresponds to the appearance of an incommensurate modulation ($\alpha'$ phase). $\alpha$-PbO forms a layer structure, and the interlayer spaces are occupied by the electronic lone pairs (E) (figure 1). The $\alpha$ phase is tetragonal ($a_T = 3.9704$ Å, $c_T = 5.022$ Å at 293 K), with the space group $P4/nmm$ ($Z = 2$). Below the critical temperature $T_I$, the tetragonal symmetry of PbO is broken as the average lattice of the incommensurate phase is orthorhombic ($a = a_T + b_T$, $b = a_T - b_T$, $c = c_T$). This results in a weak distortion, the spontaneous strain being very small ($\epsilon^s_{12} = 4.37 \times 10^{-4}$ at 2 K). The incommensurate (INC) $\alpha'$ phase is stable down to 2 K, and the superspace group is $P(C2mb)$: $(\bar{1}\bar{1}1)$ with $Z = 4$ [2].

The introduction of titanium oxide $TiO_2$ into the structure of $\alpha$-PbO was reported to be one way to synthesize big single crystals [3]. In this case a solid solution $Pb_{1-x}Ti_xO_{1+x}$, with $x$ ranging between 4.5 and 8 mol%, can be obtained with the litharge structure [4]. From a structural point of view, we have shown [4] that a $TiO_2$ group ($Ti^{4+}$) substitutes for a PbOE group, the extra oxygen atom occupying the volume of the lone pair. However, in this case [5] the INC phase is suppressed and the tetragonal phase remains to 2 K.

From the structural determination of the $\alpha'$ phase [2], it was presumed that incommensurability is due to interactions between lone pairs. This hypothesis is confirmed by the stability of the tetragonal phase in $Pb_{1-x}Ti_xO_{1+x}$ which could be interpreted by breaks in the lone-pair alignments (figure 2). In order to get a better understanding of the phase transition and phenomena which are responsible for the incommensurability, x-ray diffraction and Raman scattering investigations were carried out over a wide range of temperature in PbO and $Pb_{1-x}Ti_xO_{1+x}$ compounds.

0953-8984/95/458547+10$19.50  

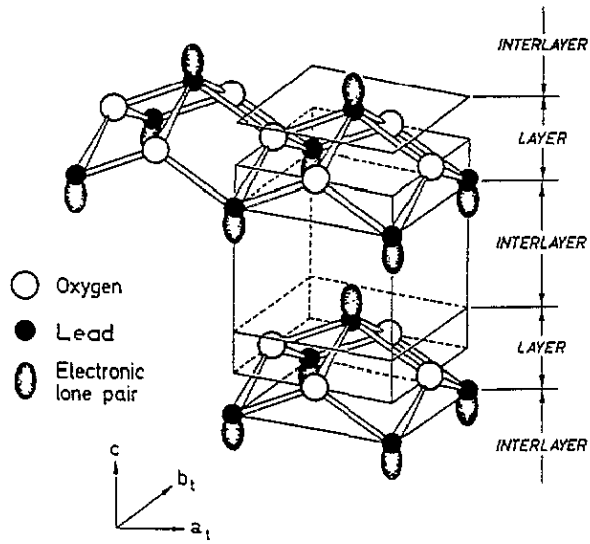


**Figure 1.** Representation of the layered structure of the $\alpha$-PbO.

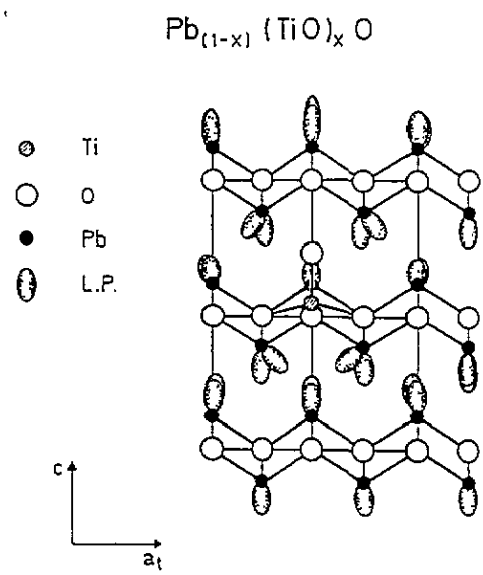


**Figure 2.** Representation of the structural model corresponding to the dissolution of $TiO_2$ in PbO. A tilt of the lone pairs (LP) due to extra Ti and O atoms is clearly observed.

## 2. Experimental details

PbO and $(PbO)_{1-x}(TiO_2)_x$ single crystals (with $x = 0.045$), obtained by hydrothermal synthesis, were used for Raman spectroscopy. Raman scattering experiments were performed using 6328 Å radiation of an He–Ne laser. The scattered light was analysed by a CODERG T800 triple monochromator with a spectral resolution of 1 $cm^{-1}$. Frequencies

and linewidths (HWHM) were determined by a fitting procedure using a damped oscillator profile. Investigations in the low-temperature range (15 K–300 K) were performed using a closed-cycle cryostat, which keeps temperature fluctuations within 0.1 K. Above room temperature a hot air stream device was used. The temperature between 310 K and 700 K is controlled within 1 K.

X-ray diffraction studies were performed on powder samples, using a two-axis goniometer with Bragg–Brentano geometry with Cu Kα monochromatic radiation from an 18 kW Rigaku rotating anode. Typical patterns from 12° to 100° ($2\theta$) were scanned through steps of 0.004 ($2\theta$) with a typical counting time of 15 s up to 120 s (for satellite peaks). During the low-temperature experiments an He cryostat with thermal stability of 0.1 K and accuracy within 1 K was used.

## 3. Results

### *3.1. X-ray diffraction*

In a previous study [6] the thermal evolution of lattice parameters was analysed in both phases of PbO. The very weak distortion was observed only through the fitting procedure of $a$ versus temperature. Here a Debye analysis of the cell parameters is reported with a classical evolution (figure 3):

$$p = p_0 + 9ART\int_0^{\theta_D/T} t^3/(e^t - 1)\,dt$$

where $p_0$ is the lattice parameter of 0 K and $\theta_0$ the Debye temperature, $R$ the perfect gas constant and $A$ a multiplicative coefficient. So the three coefficients $p_0$, $\theta_D$ and $A$ are the fitting parameters.

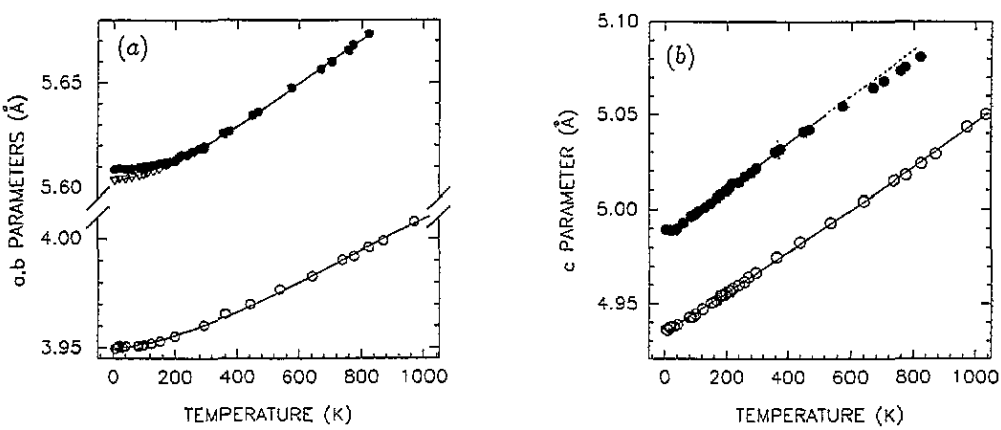


**Figure 3.** Comparison between the temperature dependence of the cell parameters in PbO (full circles) and $(PbO)_{1-x}(TiO_2)_x$ (open circles) (a) for $a$ and $b$: ($b$, open triangles); (b) for $c$. The lines correspond to the fitting procedure with the Debye law.

The thermal evolution of the $c$ parameter displays no anomaly at $T_I$ and could be fitted in the whole range of temperature (6–600 K) by a single evolution, whereas the evolution of the $a_0$ and $b_0$ parameter below $T_I$ are distinct from that of $a_T\sqrt{2}$ above $T_I$. The corresponding value of the fitting parameters $p_0$ and $\theta_D$ are in table 1, in addition to the thermal dilatation parameter $\alpha$ at 300 K. The values of the Debye temperature reveal the weak rigidity of the components of bondings in the $c$ direction ($\theta_D = 77$ K), in contrast to the components of bondings in the ($a$, $b$) plane ($\theta_D = 570$ K). This anisotropy is also revealed by the different values in the thermal dilatation at 300 K ($\alpha_c = 24 \times 10^{-6}$ K$^{-1}$ and $\alpha_a = 15 \times 10^{-6}$ K$^{-1}$).

**Table 1.** Comparison between the temperature dependence of cell parameters in both PbO and $(PbO)_{1-x}(TiO_2)_x$ compounds.

| Parameter | $\Delta T$ | $p_0$ (Å) | $\theta_D$ (K) | $\alpha \times 10^{-6}$ (K$^{-1}$) (at 300 K) |
|---|---|---|---|---|
| $a_T\sqrt{2}$(PbO) | 200 K–800 K | 5.6065(1) | 570(10) | 15(1) |
| $a_0$(PbO) | 2 K–200 K | 5.6088(1) | 250(5) | 6(1) |
| $b_0$(PbO) | 2 K–200 K | 5.6041(1) | 260(5) | 12(1) |
| $c$(PbO) | 2 K–200 K | 4.9888(1) | 77(5) | 24(1) |
| $a_I(Pb_{1-x}(TiO)_xO)$ | | 3.9504(1) | 525(5) | 15(1) |
| $c(Pb_{1-x}(TiO)_xO)$ | | 4.9368(1) | 75(3) | 22(1) |

The spontaneous strain $\epsilon_{12}$ was deduced from the thermal evolution of the $a_0$ and $b_0$ parameters; a power law $B\,(T_c - T)^m$ was fitted and gives $m = 0.77(2)$ and $T_c = 227(1)$ K. These values are very different from those obtained by Boher *et al* [6] ($m = 0.5$ and $T_c = 200$ K) and this is probably due to the absence of data in their work above 180 K. The high $m$ value suggests that the spontaneous strain could be a second-order parameter.

Figure 3 reveals a change in the slope only in the evolution of the $c$ parameter at about 550 K. This phenomenon could be interpreted as a precursor effect of the phase transition at $T_I$.

Whereas the isotypic compound $PbO_{1-x}(TiO)_xO$ does not possess a low-temperature phase transition, as no distortion of the tetragonal phase nor any satellite peaks are evidenced by diffraction techniques, it is interesting to compare the thermal evolution of the lattice parameters $a$ and $c$ in the solid solution ($x = 0.045$) with those of PbO (figure 3).

The thermal evolution of the cell parameters of $PbO_{1-x}(TiO)_xO$ was satisfactorily fitted with a Debye law over the whole range of temperature (6–600 K) (table 1). The Debye temperature and the thermal dilatation parameter $\alpha$ at 300 K are about the same as those of PbO: anisotropy between the $c$ and $a$ directions is revealed, as in PbO, by the differences both in the Debye temperatures and the thermal dilatation coefficients corresponding to these two directions.

These results show that dissolving $TiO_2$ in PbO induces a contraction of the cell parameters of the PbO tetragonal cell (at room temperature $a = 3.9665$ Å and $c = 4.9831$ Å instead of 3.9777 Å and 5.0259 Å). Moreover, this contraction is more important when perpendicular to the layer than when inside a layer ($\Delta c/c = 0.85\%$ and $\Delta a/a = 0.28\%$), resulting in an increase of the anisotropy of the structure. This anisotropic distortion is related to the presence of the extra oxygen atom in the layer, which creates new interlayer interactions Pb-O2 and Ti-O2 [4].

### *3.2. Raman scattering study*

The Raman spectrum of α-PbO at room temperature consists of only four lattice modes ($A_{1g}$ + $B_{1g}$ + $2E_g$) in accordance with group theory analysis (figure 4). Both modes corresponding to interactions between lead atoms (along *c*: $A_{1g}$, in the *ab* plane: $E_g^{(1)}$) exhibit harmonic character (via the sharpness of oscillator profiles) at room temperature, in contrast with oxygen vibrations (along *c*: $B_{1g}$, in the *ab* plane: $E_g^{(2)}$) which are characterized by broadening damped oscillator profiles.

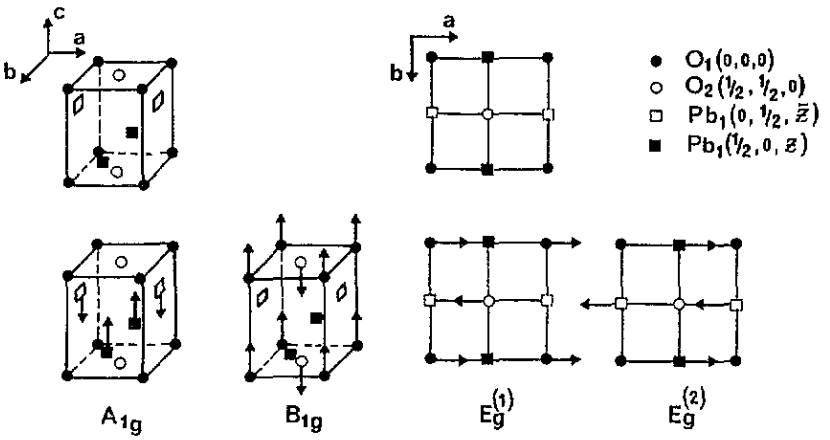


**Figure 4.** Description of the four Raman active modes in PbO.

In the α phase the temperature dependence of the frequency and linewidth (HWHM) is reported for each mode in figure 5. These figures point out a change in the slope of the frequency temperature dependence at 553 K, except for the $E_g^{(2)}$ mode. For the latter, its very weak intensity, together with a strong broadening, results in the determination of its frequency within large error bars. For this reason the points above 500 K were not reported in figure 6, and so it is not possible to conclude the observation of an anomaly at 550 K for this mode. Figure 5 and table 2 show that the change of slope at 553 K is more marked for the $E_g^{(1)}$ and $B_{1g}$ than for the $A_{1g}$ mode. From consideration of linewidths (figure 5), and with regard to the frequency shifts of lead atom vibration ($A_{1g}$ and $E_g^{(1)}$ modes), the strongest temperature dependence ($A_{1g}$) is not associated with the strongest change of slope. Consequently, the magnitude of the change in the slope of each mode is certainly dependent on a change in their anharmonic behaviour caused by a structural modification in the (*a*, *b*) plane.

Below 550 K in the α phase, figure 6 and table 2 show a strong temperature dependence of the $E_g^{(2)}$ mode frequency, certainly induced by the anharmonic behaviour of this mode. The evolution of this mode could be correlated to a hardening of the Pb–O bonds which are approximately in the plane where O–O interactions (corresponding to the $E_g^{(2)}$ mode) are involved.

At $T_I$, a very marked change of the frequency temperature dependence is observed only for the $E_g^{(2)}$ mode (figure 6(a)). This phenomenon seems to be connected to a discontinuity in the evolution of the corresponding linewidth and therefore to a strong sharpening of the phonon peak below $T_I$ (figure 6(b)). However, the lattice distortion is not observed via

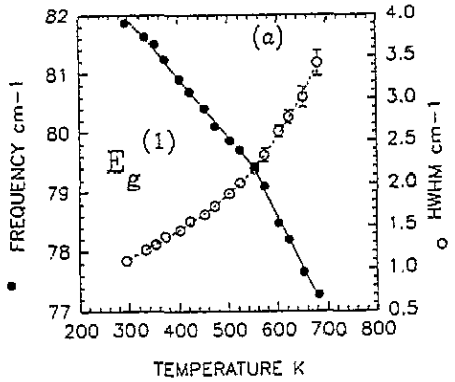


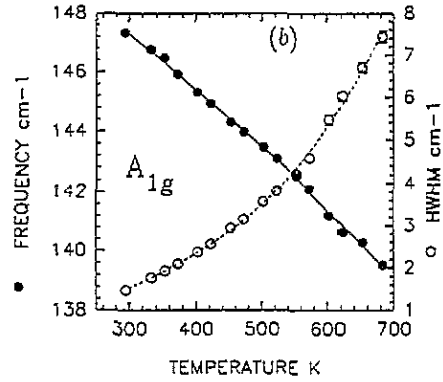


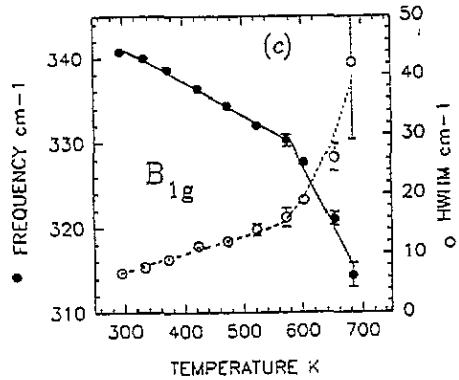


**Figure 5.** Temperature dependence of the frequency and linewidth in PbO for the $E_g^{(1)}$ mode (a); the $A_{1g}$ mode (b); $B_{1g}$ mode (c). The circles represent experimental data whereas full and dashed lines correspond to fitted data with first-order (frequency) and third-order (linewidth) regressions.

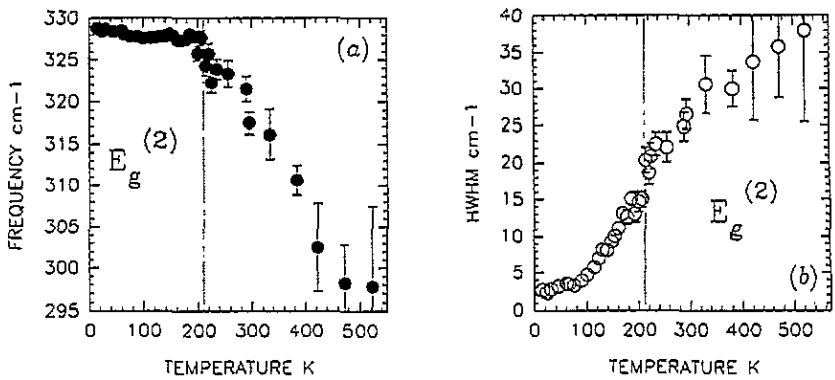


**Figure 6.** Temperature dependence of $\nu(E_g^{(2)})$ (a) and the corresponding *HWHM* (b).

the behaviour of this mode, in contrast to the $E_g^{(1)}$ mode which corresponds to interactions between lead atoms in the ($a$, $b$) plane. This latter splits below $T_I$ (figure 7(a)) and so gives rise to a very weak component, whereas the frequency shift versus temperature of the first component does not undergo any break. The $A_{1g}$ and $B_{1g}$ modes, involving interactions along $c$, do not exhibit any anomaly at $T_I$ either in the frequency or linewidth temperature dependences.

**Table 2.** Temperature dependence of the frequencies corresponding to the four Raman active modes in PbO and $(PbO)_{1-x}(TiO_2)_x$. The reported values are obtained from fitting the linear temperature dependence of the frequency between 300 K and 700 K with a first-order regression.

| | $\partial\nu/\partial T$ ($cm^{-1}$ $K^{-1}$) for PbO | | | $\partial\nu/\partial T$ ($cm^{-1}$ $K^{-1}$) for $(PbO)_{1-x}(TiO_2)_x$ | |
|---|---|---|---|---|---|
| Modes | 300 K | 550 K | 700 K | 300 K | 700 K |
| $A_{1g}$ | −0.019(1) | −0.023(1) | | −0.019(1) | |
| $B_{1g}$ | −0.039(3) | −0.143(6) | | −0.039(1) | |
| $E_g^{(1)}$ | −0.010(1) | −0.170(7) | | −0.009(1) | |
| $E_g^{(2)}$ | −0.105(3) | — | | — | |

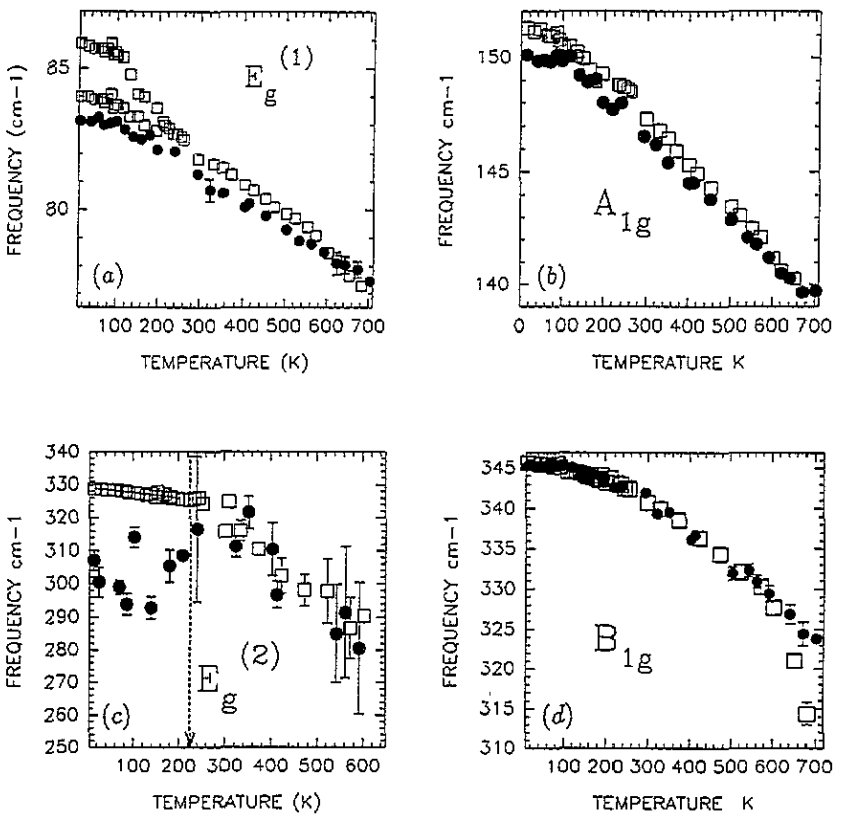


**Figure 7.** Comparison of the temperature dependence of the four Raman active modes in both PbO and $(PbO)_{1-x}(TiO_2)_x$; $E_g^{(1)}$ (a), $A_{1g}$ (b), $E_g^{(2)}$ (c) and $B_{1g}$ (d). The open squares correspond to frequencies observed in PbO, and the filled circles to those observed in $(PbO)_{1-x}(TiO_2)_x$.

Addition of $TiO_2$ into PbO induces some modifications of the Raman scattering spectrum, as given below.

(i) The appearance of new phonon peaks corresponding to interactions between layers (Pb–O → $\nu = 185$ $cm^{-1}$ at room temperature) and inside the layers (Ti–O). Because of its influence on the cohesion between the layers, the temperature dependence of the 185 $cm^{-1}$ peak was analysed (figure 8). The hard frequency shift of this mode versus temperature in the high-temperature range is certainly responsible for the enhancement of anisotropy in

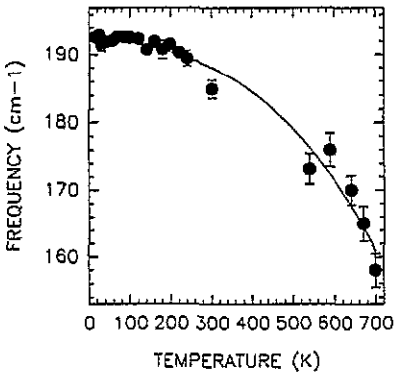


**Figure 8.** The temperature dependence of the 185 $cm^{-1}$ mode frequency in $(PbO)_{1-x}(TiO_2)_x$.

this compound.

(ii) The four $A_{1g}$, $B_{1g}$ and $E_g$ modes are broader in the solid solution than in $\alpha$-PbO at room temperature. This observation can be interpreted by the coexistence of several configurations characterized by different interatomic distances (Pb–Pb or O–O) due to $TiO_2$ addition. However, the temperature dependence of the linewidths is stronger in $\alpha$-PbO above 500 K. This phenomenon is significantly observed for the ($A_{1g}$ and $B_{1g}$) modes involving (Pb–Pb and O–O) interactions along *c*.

(iii) The frequencies of $A_{1g}$, $E_g^{(1)}$ and $E_g^{(2)}$ modes are systematically lower in $(PbO)_{1-x}(TiO_2)_x$ below 550 K. Above this temperature the opposite phenomenon is observed for $A_{1g}$ and $E_g^{(1)}$, because of the change in the frequency shifts at 550 K in PbO. However, the $B_{1g}$ frequencies are systematically superposed in both compounds between 15 K and 550 K, and above 550 K the frequency becomes lower in PbO in a significant way. This could indicate that the anomaly observed in PbO at 550 K could result from structural modification inside the layers, the $B_{1g}$ mode involving only interactions inside the layers as a notable contribution in the potential function. In contrast, the potential associated with the $A_{1g}$ mode has a component dependent on second-nearest lead atoms involving interlayer interactions.

(iv) The temperature dependences of $A_{1g}$, $B_{1g}$ and $E_g^{(1)}$ frequencies are observed as in PbO below 550 K. However, strong differences are pointed out in the behaviour of the $E_g^{(2)}$ mode in both compounds. In the solid solution, this mode seems to be temperature independent, like an internal-mode behaviour.

## 4. Discussion and conclusion

X-ray diffraction and Raman scattering data show a very good accordance and reveal some common features.

(i) The thermal expansion of the *c* parameter, corresponding essentially to the thermal expansion of the interlayer space [5], is stronger than that of the *a* parameter. This characteristic is also observed from Raman scattering experiments through the comparison of frequency shifts versus temperature for $A_{1g}$ and $E_g^{(1)}$, involving interactions between lead atoms along *c* and in the *a*, *b* plane.

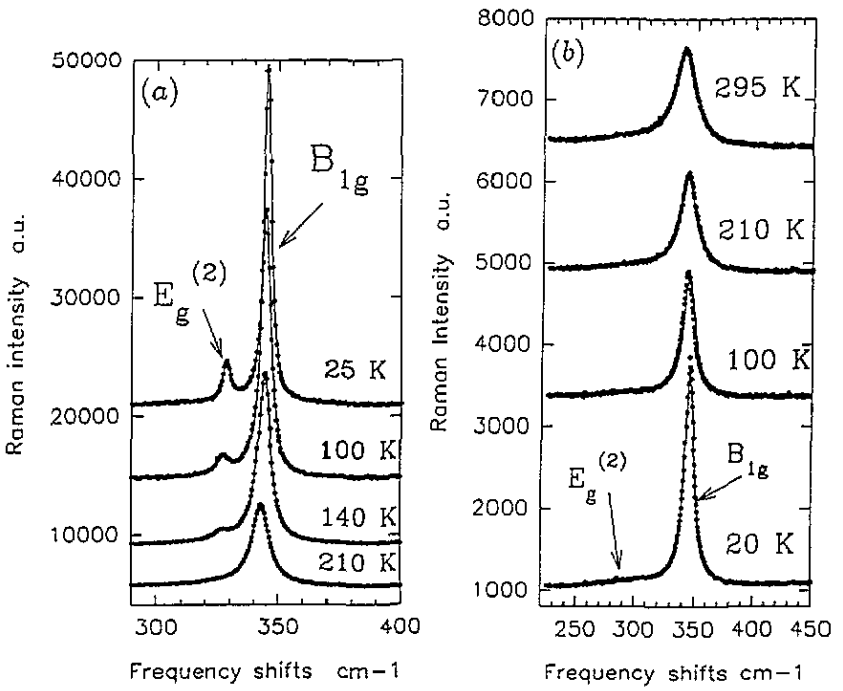


**Figure 9.** Comparison of the temperature dependence of the $E_g^{(2)}$ mode (a) in PbO and (b) in $(PbO)_{1-x}(TiO_2)_x$.

(ii) The thermal expansion of the lattice parameters is observed to be very similar in both compounds. The temperature dependence of the Raman frequencies below 550 K also exhibits this behaviour, except for the $E_g^{(2)}$ mode.

However, Raman spectroscopy experiments point out some additional information about the anomaly at 550 K and the phase transition at 208 K observed in PbO.

(iii) The anisotropic character of the layered structure is revealed from the Debye analysis of the lattice parameters ($\theta_D = 570$ K in the $a$, $b$ plane, and $\theta_D = 77$ K along $c$). On the other hand, frequencies are lower for vibrations in the ($a$, $b$) plane than vibrations along $c$. This observation can be interpreted in terms of electrostatic potentials in which repulsive interactions between lone pairs have a great contribution. This contribution is only in relation to second-nearest lead atoms pointing towards each other [7], and consequently principally modifies the potential constant of interlayer interactions between lead atoms.

(iv) The dissolution of $TiO_2$ involves a contraction of the cell parameters. However, a lowering of the $A_{1g}$ and $E_g^{(1)}$ frequencies is observed below 550 K in $(PbO)_{1-x}(TiO_2)_x$. This could be interpreted as a weaker contribution of lone-pair interactions in the solid solution, caused by extra interactions (Pb–O) between the layers, and by substitution of Pb–E entities with Ti–O groups.

(v) The anomaly at 550 K in PbO is observed via the behaviour of several modes involving atomic vibrations along $c$ and perpendicular to $c$, whereas only the thermal dilatation of the $c$ parameter exhibits a special behaviour at this temperature. From comparison of the magnitudes in the manifestation of this phenomenon through the behaviour of the $A_{1g}$ (involving interactions inside and between the layers) and $B_{1g}$ (interactions inside the layer) frequencies and the lack of dependence of the $B_{1g}$ frequency

on $TiO_2$ addition below 550 K (table 2, figure 7(d)), it can be assumed that structural modifications take place inside the layer at 550 K. These modifications seem to induce a contraction of the layer via the increasing of the lone-pair interactions, and then an enhancement of the anisotropy of the PbO structure. This interpretation confirms the precursor effect assigned to the anomaly at 550 K, which certainly corresponds to the origin of the $E_g^{(2)}$ mode behaviour.

(vi) A striking phenomenon, evidenced from Raman scattering experiments, is the contrasting behaviour of the $E_g^{(2)}$ modes in both compounds (figures 7(c) and 9). Because of the stronger contraction of the *a* parameter (in proportion to the O–O distances [6]) in $(PbO)_{1-x}(TiO_2)_x$, and the internal mode behaviour of $E_g^{(2)}$ in this compound, the very strong temperature dependence of this mode in $\alpha$-PbO seems to be very closely connected with the phase transition. From the similarity between the thermal expansion of the *a* parameter in both compounds, it can be assumed that the behaviour of $E_g^{(2)}$ is caused by an external force field, such as the interactions between lone pairs. The hard frequency shift of the mode, together with the strong decreasing of the linewidth versus temperature, reveals a hardening of the O–O interactions which could be the origin of the lattice break. The stability of the tetragonal structure can be understood from the consideration of the extra interlayer Pb–O interactions which keep the lone-pair interactions constant.

The comparative study of PbO and $(PbO)_{1-x}(TiO_2)_x$ has revealed the consequences of considering electronic lone-pair interactions to the understanding of the anomaly at 550 K and the phase transition process in PbO. In order to give a more precise relationship between the behaviour of the $E_g^{(2)}$ mode and the phase transition, it would be interesting to perform Raman scattering studies of different *x*-values and the isostructural compound SnO.

## References

[1] Moreau J, Kiat J M, Garnier P and Calvarin G 1989 *Phys. Rev.* B **39** 10296
[2] Hedoux A, Grebille D and Garnier P 1989 *Phys. Rev.* B **40** 10653
[3] Oka K, Unoki H and Sakuto T 1979 *J. Cryst. Growth* **47** 568
[4] Moreau J, Boher P and Garnier P 1989 *Mater. Res. Bull.* **24** 1241
[5] Le Bellac D 1993 *Thèse* Université de Paris XI, Orsay
[6] Boher P and Garnier P 1986 *C. R. Acad. Sci. Paris* II **298** 6; 1993 *Thèse* Université de Paris XI, Orsay
[7] Donaldson J D, Donoghue M T and Ross S D 1974 *Spectrochim. Acta* A **30** 1967